

Supplementary Information

A Favored Crystal Orientation for Efficient Printable Mesoscopic Perovskite Solar Cells

*Jiawen Wu,^a Weihua Zhang,^a Qifei Wang,^a Jiankang Du,^a Shuang Liu,^a Anyi Mei,^a Yaoguang Rong,^a Yue Hu,^{*a} Hongwei Han^a*

^a Michael Grätzel Center for Mesoscopic Solar Cells, Wuhan National Laboratory for Optoelectronics, Huazhong University of Science and Technology, Wuhan 430074, Hubei, PR China

*Addresses correspondence to: E-mail:

yuehu@hust.edu.cn

EXPERIMENTAL DETAILS

Materials and perovskite precursor solutions preparation

Unless otherwise specified all materials were purchased from Sigma-Aldrich. Lead iodide (PbI_2), anhydrous dimethylformamide (DMF) and anhydrous dimethyl sulfoxide (DMSO) were purchased from Sigma-Aldrich and used without further purification. To prepare the pristine perovskite precursor solution, MAI and PbI_2 powder were mixed in anhydrous solvent (DMF: DMSO = 4:1) with a molar ratio of 1 : 1.

MAPbI₃ perovskite precursor solution: 0.159 g MAI powder and 0.461 g PbI_2 powder were mixed in mixture solvent of 800 μL DMF and 200 μL DMSO. The solutions were transferred onto a magnetic stirring apparatus stirred overnight at room temperature (400 r/min).

GA-MAPbI₃/DMBG-MAPbI₃/BH-MAPbI₃ perovskite precursor solution: 0.159 g MAI powder, 0.461 g PbI_2 powder and different molar ratios of GA, DMBG, BH powder were mixed in mixture solvent of 800 μL DMF and 200 μL DMSO (The molar ratio of GA/DMBG/BH: PbI_2 is 10%, 20%, 30% and 40%). The solutions were transferred onto a magnetic stirring apparatus stirred overnight at room temperature (400 r/min).

Preparation of TiO₂ slurry

3.0 g TiO₂ raw material (Dyesol NR-30) was added into 12.0 g terpineol, then transferred onto a magnetic stirring apparatus stirred 12 h at room temperature (400 r/min).

Preparation of ZrO₂ slurry

10 g ZrO₂ nanopowders (particle size: 20 nm) was added in a 30 mL terpineol solution, and 1 g of ethyl cellulose were added into solution, followed by stirring vigorously using ball milling for 2 h.

Preparation of carbon slurry

2g carbon black powders (particle size: 30 nm) was mixed with 6 g graphite powders in a 30 mL terpineol solution, and then 1 g of 20 nm ZrO₂ nanopowders and 1 g of ethyl cellulose were added into solution, followed by stirring vigorously using ball milling for 2 h.

Fabrication of Perovskite Solar Cells

The FTO conducting glass was etched with a laser to form desired electrode patterns before being ultrasonically cleaned with a detergent solution, deionized water, and ethanol for 15 min, respectively. A compact layer of TiO₂ was deposited on the FTO-coated glass by spray pyrolysis deposition at 450 °C with diisopropoxide bis (acetylacetonate) solution and sintered for 30 min. deposited on top of the compact layer by screen printing and then sintered at 500 °C for 30 min. After cooling down to room temperature naturally, a 500 nm mesoporous TiO₂ layer was deposited on top of the compact layer by screen printing use TiO₂ slurry and then sintered at 500 °C for 30 min. After then, a 3 μm ZrO₂ spacer layer and a 15 μm carbon layer were subsequently screen-printed on the top of the TiO₂ layer, and then the films were sintered at 400 °C. The equipment used for 500 °C and 400 °C sinter process is muffle furnace. And the pressure of screen printing is 0.75 kg. Then take the cells off from the hot plate and cooling down to room temperature. After that, a 3.5 μL of perovskite precursor solution

was dipped on the mesoporous carbon layer, followed by annealing at 100 °C for 20 min. The active area of each device is 0.8 cm².

Sample preparation

UV-Vis, XRD, SEM , steady-PL and GIWAX: Drop 0.5 μL of perovskite precursor solution onto the mesoporous TiO₂ layer followed by annealing at 100 °C for 20 min.

TRPL: Drop 0.5 μL of perovskite precursor solution onto the mesoporous ZrO₂ layer followed by annealing at 100 °C for 20 min.

UPS and XPS: The perovskite precursor solutions was spin-coated onto the precleaned ITO at 4000 rpm for 30 s, and annealed at 100 °C for 20 min.

Stability measurement

Environmental stability: The devices was stored in the dark boxes in ambient atmospheric which humidity is 50 ± 5% RH.

Thermal stability: The devices was stored in the gloves boxes in N₂ atmospheric.

Characterization

The ¹H NMR spectra were measured with Ascend™ 600 MHz nuclear magnetic resonance spectrometer. The morphology of samples was observed by a field-emission scanning electron microscope (SEM) (FEI Nova NanoSEM450). The mesoscopic film thickness was measured by using a profilometer (Dektak XT, Brucker). The XRD spectra were measured with an X'pert PRO X-ray Diffractometer using Cu Kα radiation under operating conditions of 40 kV and 40 mA from 5° to 70°. The XPS was measured by ESCALAB 250Xi X-ray photoelectron spectroscopy. Device performance was characterized by a Keithley 2400 source/meter and a Newport solar simulator (model

91192) which offered the simulated AM 1.5G illumination of 100 mW cm^{-2} , calibration was done using a NIST-certified monocrystalline Si solar cell (Newport 532 ISO1599). The J - V curves have measured by reverses scan (1.2 V to -0.2 V) with a scan rate of 10 mV s^{-1} . A mask with a circular aperture (0.101 cm^2) was applied for J - V measurements. Incident photo-to-current conversion efficiency was performed using a 150 W xenon lamp (Oriel) fitted with a monochromator (Cornerstone 74004) as a monochromatic light source. Time-resolved photoluminescence (TRPL) decay transients were measured at 780 nm using excitation with a 478 nm light pulse from a HORIBA Scientific DeltaPro fluorimeter. The UPS was measured by ESCALAB 250Xi Ultraviolet electron. The UV-vis was measured by using a SolidSpec-3700 Ultraviolet-visible near-infrared spectrophotometer. The steady-state photoluminescence (PL) spectra were taken on a Horiba JobinYvon LabRAM HR800s with a 532 nm wavelength excitation source. GIWAXS measurements were conducted at the BL14B1 beamline of the Shanghai Synchrotron Radiation Facility(SSRF). The incident photon energy was 18 keV (wavelength= 0.688 \AA) and the two-dimensional GIWAXS patterns were acquired by a 2D MarCCD detector. The incidence angle of 1.2° was adopted to achieve depth-dependent information with an exposure time of 40 s. The sample-to-detector distance was 452.8mm, calibrated with a lanthanum hexaboride (LaB_6) sample. The X-ray scattering data were processed and analyzed with the software FIT2D and displayed in scattering vector q coordinates.

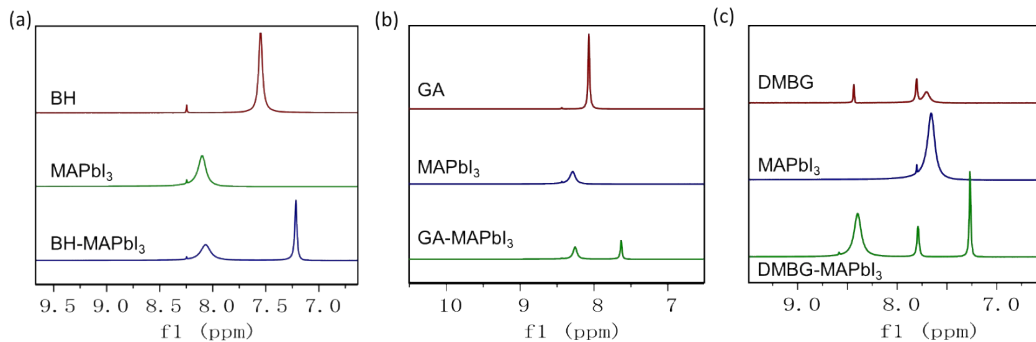


Figure S1. (a) ¹H NMR of BH, MAPbI₃, and BH-MAPbI₃. (b) ¹H NMR of GA, MAPbI₃ and GA-MAPbI₃. (c) ¹H NMR of DMBG, MAPbI₃ and DMBG-MAPbI₃. The BH, GA, DMBG sample was prepared by dissolving 0.15 mM BH, GA, DMBG in 0.5 ml DMF-d₇. The MAPbI₃ sample was prepared by dissolving 0.5 mM PbI₂ and 0.5 mM MAI in 0.5 ml DMF-d₇. BH-MAPbI₃, GA-MAPbI₃, DMBG-MAPbI₃ sample was dissolving 0.15 mM BH, GA, DMBG with 0.5 mM MAI and 0.5 mM PbI₂ in 0.5 ml DMF-d₇.

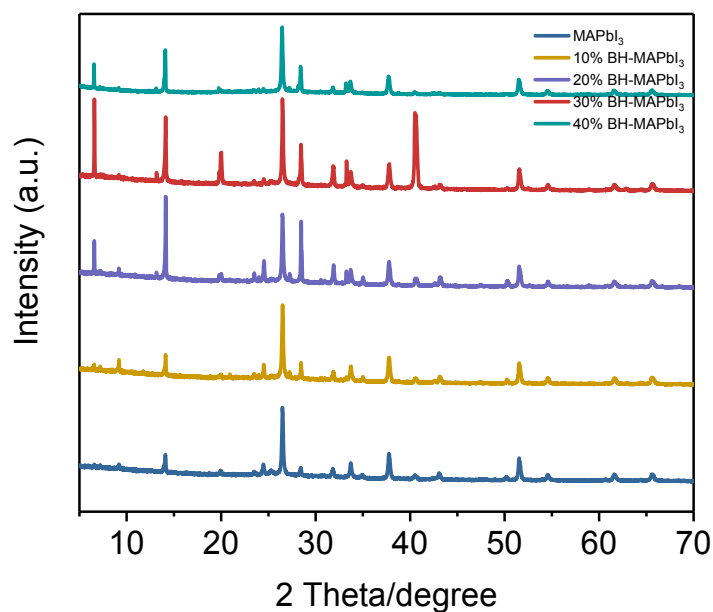


Figure S2. XRD characterization of 10% BH-MAPbI₃, 20% BH-MAPbI₃, 30% BH-MAPbI₃, and 40% BH-MAPbI₃ perovskite films prepared on mp-TiO₂.

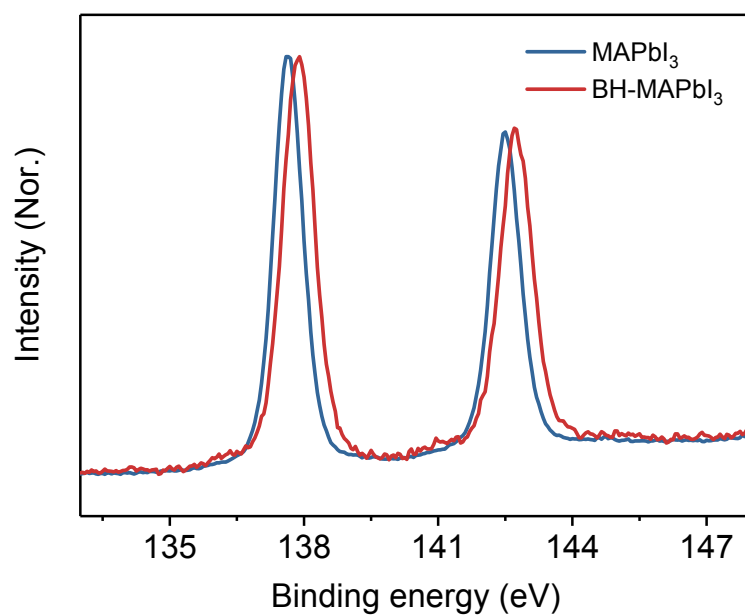


Figure S3. Pb 4f orbit of the MAPbI₃ and BH-MAPbI₃.

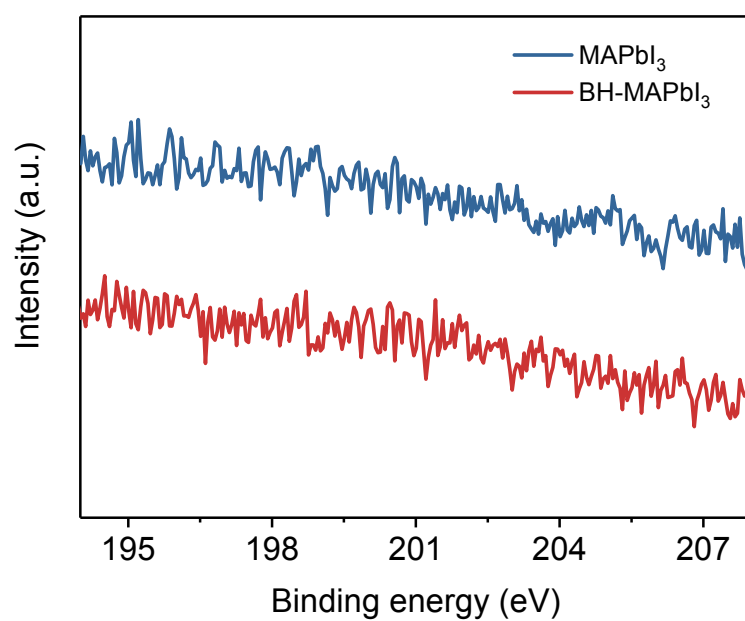


Figure S4. Cl 2p orbit of the MAPbI₃ and BH-MAPbI₃.

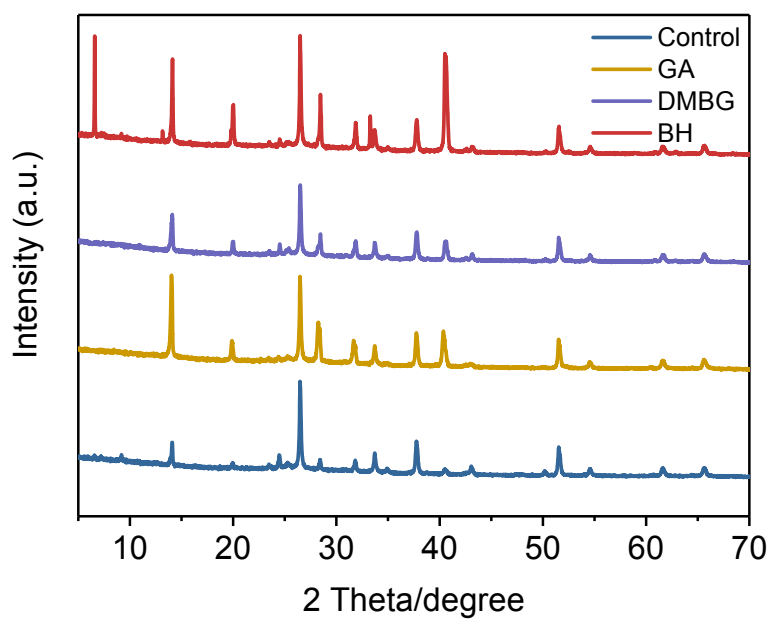


Figure S5. XRD characterization of MAPbI₃, GA-MAPbI₃, DMBG- MAPbI₃, BH- MAPbI₃ perovskite thin films on mp-TiO₂.

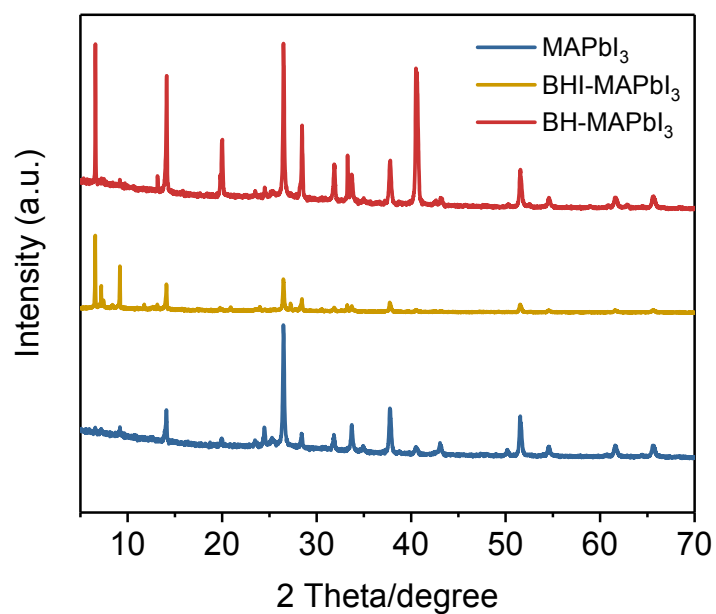


Figure S6. XRD characterization of MAPbI₃, BHI-MAPbI₃ and BH- MAPbI₃.

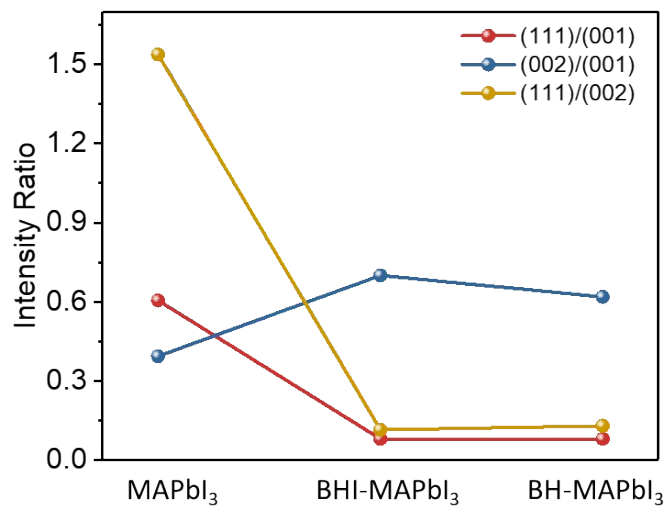


Figure S7. Intensity ratios of different crystal planes of perovskite thin films with BHI and BH.

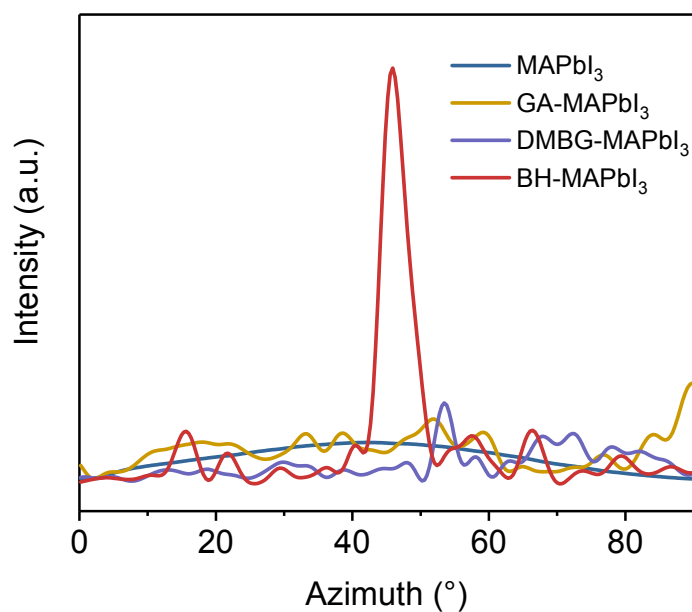


Figure S8. Integrated GIWAXS intensity plots azimuthally along the ring at $q = 10 \text{ nm}^{-1}$, with different guanidine salts, assigned to the (001) plane of corresponding perovskite films.

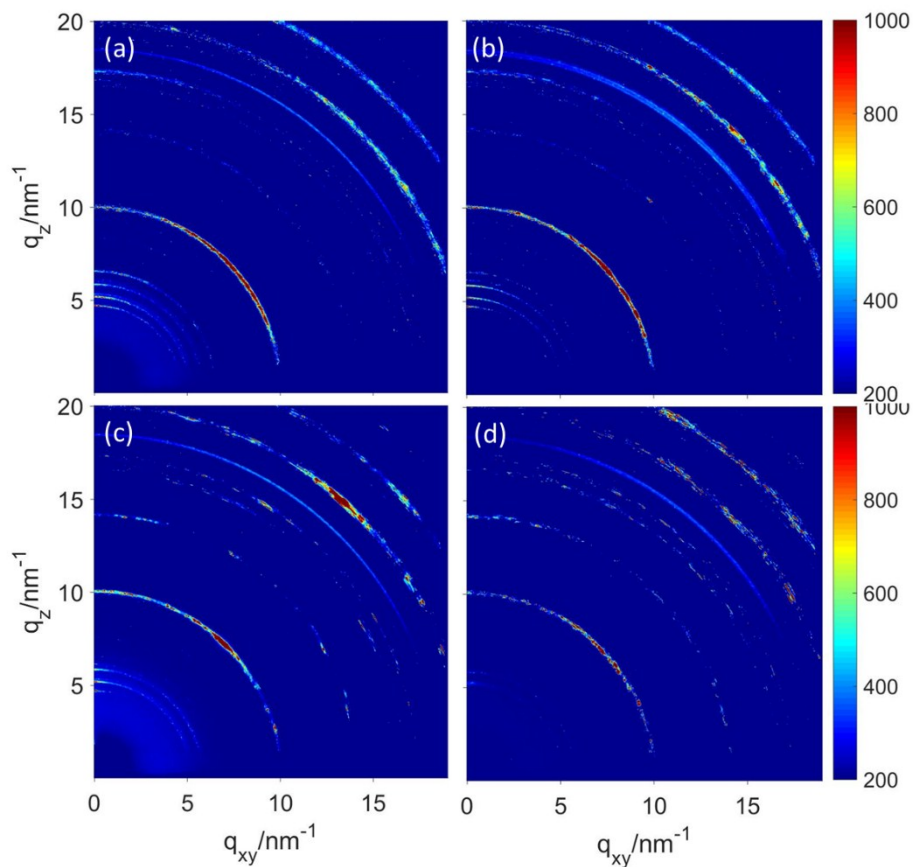


Figure S9. (a)-(d) GIWAXS of 10% BH-MAPbI₃, 20% BH-MAPbI₃, 30% BH-MAPbI₃, 40% BH-MAPbI₃ perovskite films prepared on mp-TiO₂.

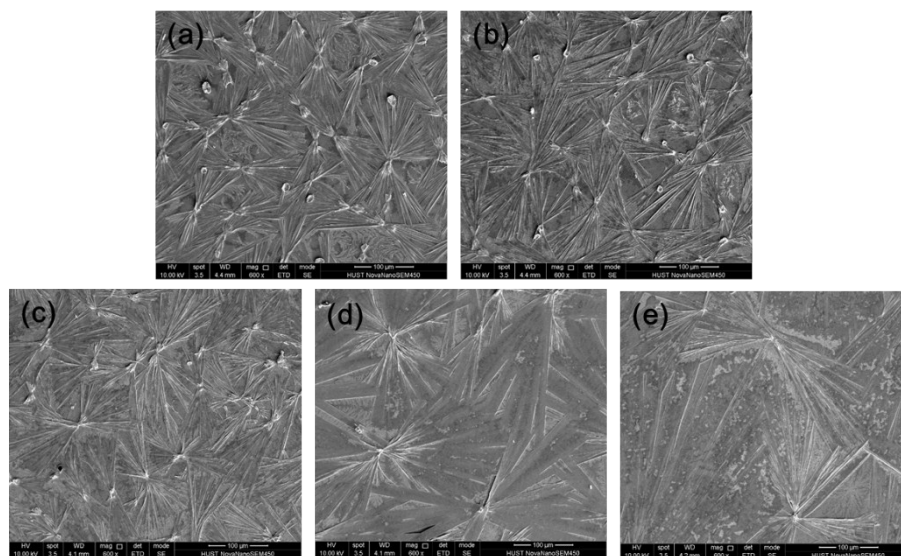


Figure S10. Top-view SEM of (a) MAPbI₃. (b) 10% BH-MAPbI₃. (c) 20% BH-MAPbI₃. (d) 30% BH-MAPbI₃. (e) 40% BH-MAPbI₃.

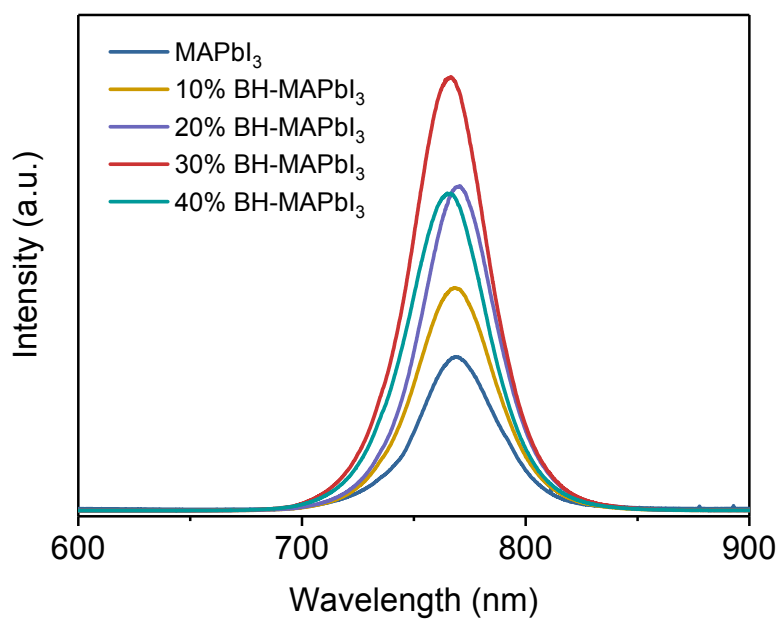


Figure S11. Comparison of the steady-state PL intensities of MAPbI₃, 10% BH-MAPbI₃, 20% BH-MAPbI₃, 30% BH-MAPbI₃ and 40% BH-MAPbI₃ films deposited on ZrO₂/glass substrates.

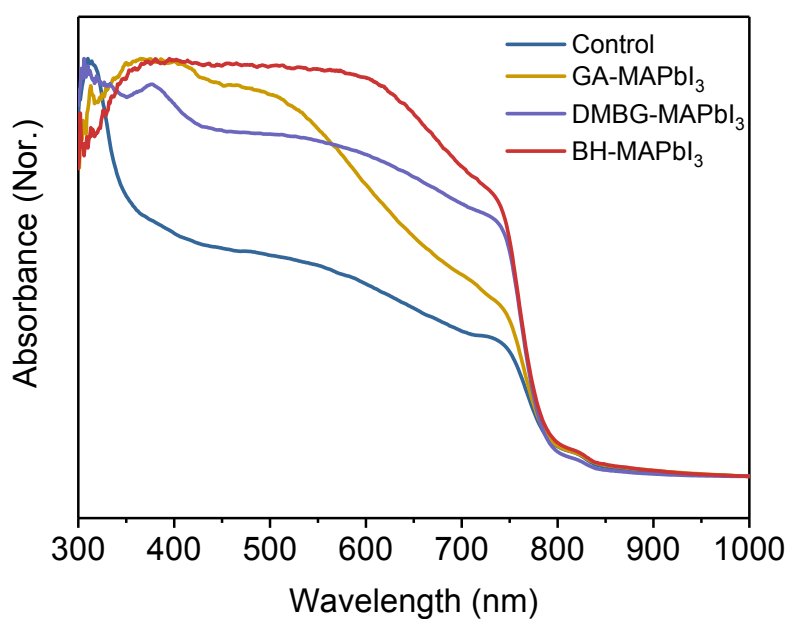


Figure S12. Normalized UV-Vis absorption spectrum of MAPbI₃, GA-MAPbI₃, DMBG-MAPbI₃ and BH-MAPbI₃.

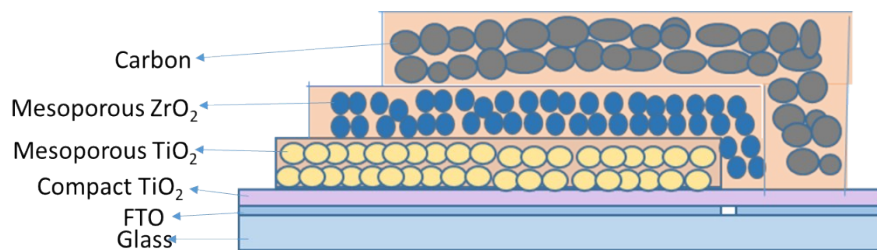


Figure S13. Schematic of the triple-layer printable mesoscopic perovskite solar cell.

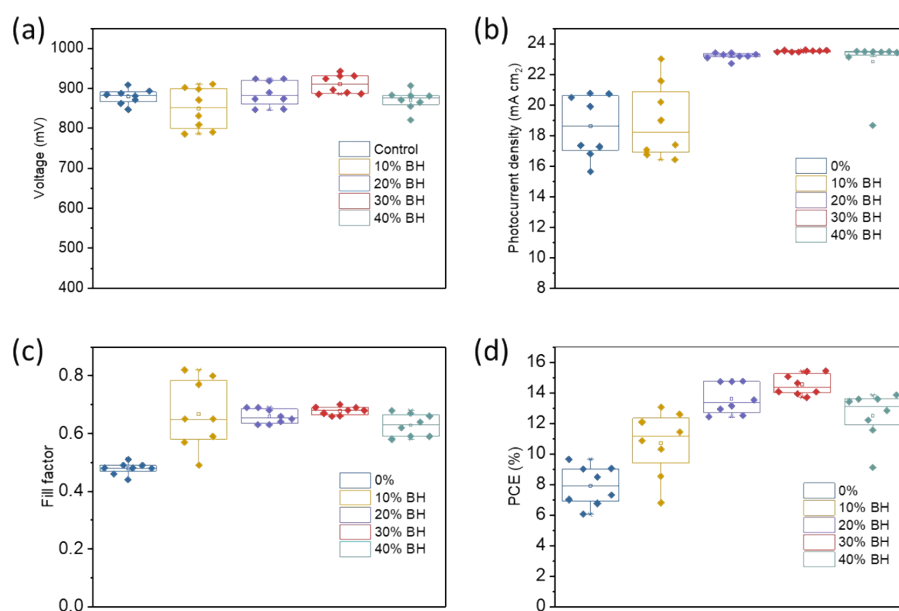


Figure S14. The parameters of devices with different concentrations of BH.

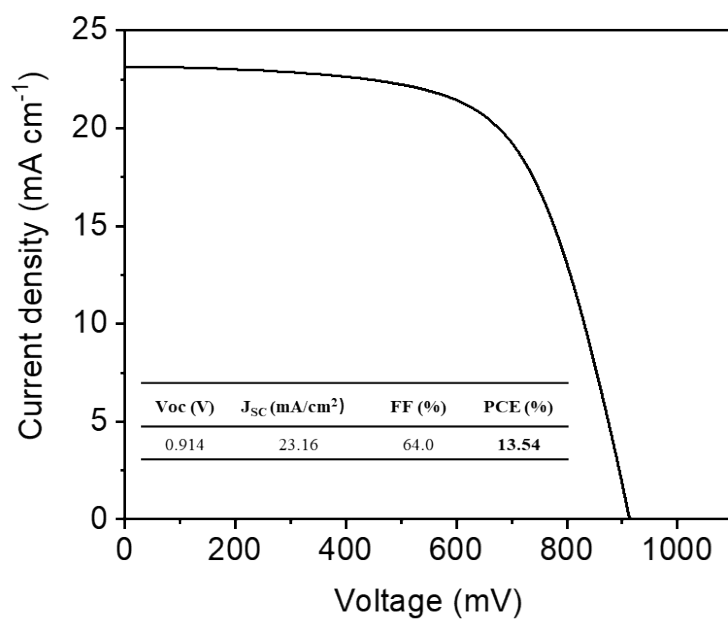


Figure S15. J - V curve of the optimized BHI-MAPbI₃.

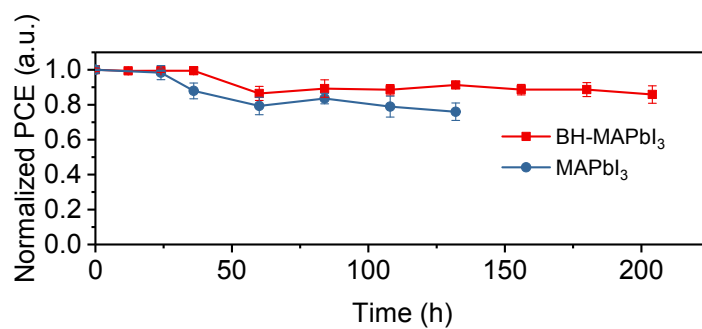


Figure S15. Thermal stabilities of device prepared by BH-MAPbI₃ and MAPbI₃. (heating at 60°C in nitrogen conditions without any encapsulation).

Table S1. Lifetimes of MAPbI₃, GA-MAPbI₃, DMBG- MAPbI₃ and BH-MAPbI₃ films deposited on ZrO₂/glass substrates.

Entry	τ_1 (ns)	τ_2 (ns)	B1	B2	Lifetimes (ns)
MAPbI ₃	9.79	31.17	0.467	0.533	21.19
GA-MAPbI ₃	8.97	52.13	0.472	0.528	31.77
DMBG- MAPbI ₃	19.84	56.38	0.403	0.597	41.65
BH-MAPbI ₃	19.14	86.28	0.081	0.919	80.84

Table S2. Lifetimes of 10%, 20%, 30%, 40% BH-MAPbI₃ films deposited on ZrO₂/glass substrates.

Entry	τ_1 (ns)	τ_2 (ns)	B1	B2	Lifetimes (ns)
MAPbI ₃	9.79	31.17	0.467	0.533	21.19
10% BH-MAPbI ₃	11.63	31.88	0.305	0.695	25.70
20% BH-MAPbI ₃	16.11	47.22	0.253	0.747	39.35
30% BH-MAPbI ₃	19.14	86.28	0.081	0.919	80.84
40% BH-MAPbI ₃	19.86	68.41	0.148	0.852	61.22

Table S3. The parameters of different devices.

Device	Voc (V)	J_{SC} (mA/cm²)	FF (%)	PCE (%)
Control	0.908	20.72	51.3	9.65
GA-MAPbI₃	0.905	19.48	76.4	13.47
DMBG-MAPbI₃	0.907	23.35	68.1	14.43
BH-MAPbI₃	0.962	23.87	71.2	16.35